APPLIED PHYSICS

Graphene for Terahertz Applications

The optoelectronic properties of graphene are being explored for possible use in plasmonics and metamaterials at terahertz frequencies.

Philippe Tassin[1], Thomas Koschny[1], Costas M. Soukoulis[1,2]

Graphene is a one-atom-thick sheet of carbon atoms arranged in a honeycomb lattice. First obtained by exfoliation of graphite in 2004 (*1*), graphene has since evolved into a thriving research topic because of its attractive mechanical, thermal, and electrical properties (*2*–*4*), particularly the exceptionally high electron mobility. Such properties promise to revolutionize many applications (*2*–*4*), ranging from solar cells and light-emitting devices to touch screens, photodetectors (*4*), microwave transistors (*5*), and ultrafast lasers (*6*). We discuss here a number of special qualities of graphene that also make it desirable for devices manipulating terahertz waves.

The single layer of carbon atoms enables device miniaturization down to the atomic length scale. The tunable electrical properties, realized by raising or lowering the Fermi level, allow for unprecedented tunability of electromagnetic structures made of this material. The electric response of a graphene sheet is highly reactive, resulting in the existence of strongly localized, deeply subwavelength plasmons (collective electronic excitations), as well as the reduction of the resonance frequency of resonant structures made of patterned graphene that allows these resonators to be made much smaller than their resonance wavelengths. Also, with optical excitation, it is possible to create an inversion of the whole conical electronic band around the Dirac point up to the pump frequency, which should afford sizable broadband gain from terahertz to optical frequencies.

Although there are abundant estimates from simplified theoretical models and experimental data for the DC properties of graphene from transport measurements, experimental data on the terahertz properties, especially the complex optical sheet conductivity, have become available only in the past few years. These data are essential to assess the potential performance of graphene in its various envisioned applications (*7*). The sheet resistivity (the real part of the inverse complex sheet conductivity) determines the loss, which relates to the dissipative quality factor of graphene-based metamaterials, as well as the propagation length of surface plasmons. The sheet inductivity (the imaginary part of the inverse complex sheet conductivity divided by the angular frequency) determines the confinement or kinetic inductance, which translates to the saturation frequency—or maximum resonance frequency—of small-scale metamaterial resonators, as well as to the "subwavelengthness" and lateral confinement of the surface plasmons.

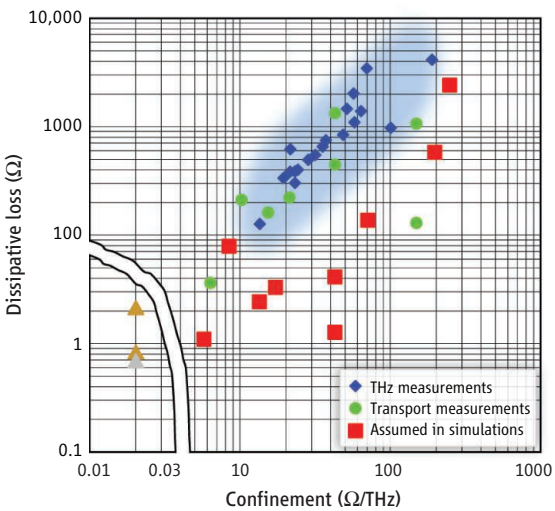

How graphene measures up. Overview of the sheet conductivity of graphene classified according to the dissipative loss and the confinement as found in current literature [detailed data are provided in the supplementary materials (*15*)].

We surveyed direct experimental measurements of the terahertz sheet conductivity of graphene found in the literature (see the figure, blue diamonds) (*8*–*11*). Select experimental data from transport measurements (green circles) are shown for comparison. Theoretical investigations of potential graphene applications have chosen different, mostly very optimistic, assumptions (red squares) for the sheet conductivity. Notably, the theoretical loss estimates are generally about one order of magnitude below the experimental data. For reasonable carrier densities, these theoretical studies obtain interesting device behavior if the sheet resistivity is roughly 100 ohms or smaller (*12*, *13*). Much effort has been directed to producing pristine samples and, indeed, suspended graphene (minimizing disorder and phonons originating from the substrate), cleaned in situ by heating, has shown impressive mobilities exceeding 10^5 cm^2/V·s, but at the expense of very limited carrier concentrations. On the other hand, large doping levels have been demonstrated by electrolytic gating, but this has led to much higher scattering.

Interestingly, the experimental data line up within a rather narrow corridor (shaded blue), indicating that the variance in carrier concentration roughly trades higher confinement for higher loss in existing graphene samples. However, this observation should not be considered to indicate a particular dependence of the momentum relaxation time on carrier concentration, as the available samples differ substantially from one another. Nevertheless, it illustrates the current discrepancy between the experimentally realizable and the theoretically desired performance.

For metamaterial applications, graphene has to compete with metals. A 30-nm film of gold (*7*) has an experimentally measured sheet resistivity on the order of 1 ohm [yellow (Au) and gray (Ag) triangles in the figure], two orders of magnitude smaller than the theoretical lower limit of 30 ohms for free-standing graphene at room temperature (*14*). The miniaturization advantage of graphene is marginal at terahertz frequencies, because the gold film is still much thinner than the free-space wavelength, and other constraints (e.g., minimum area to maintain a useful magnetic moment) require larger unit cells. However, a major drawback of metals is their lack of control over carrier density. Graphene offers a substantial advantage as its properties can be readily tuned by applying a gate voltage.

For plasmonics, the main challenge is the short propagation length in graphene that is on the order of a few surface plasmon wavelengths at best in state-of-the-art experiments. However, tunability and confinement,

[1]Ames Laboratory–U.S. Department of Energy and Department of Physics and Astronomy, Iowa State University, Ames, IA 50011, USA. [2]Institute of Electronic Structure and Lasers (IESL), FORTH, 71110 Heraklion, Crete, Greece. E-mail: soukoulis@ameslab.gov

Published by AAAS

in particular, may outweigh this limitation in the terahertz region as there are few alternatives (plasmon confinement on metals is very poor below optical frequencies).

Graphene is a fascinating material for terahertz applications with its strengths in atomic thickness, easy tunability, and high kinetic inductance. The major challenge for these resonant high-frequency applications remains to overcome the dissipative loss, which might be less of a disadvantage for surface plasmonics on graphene than for graphene as a substitute for metals in metamaterials.

References and Notes

1. K. S. Novoselov *et al*., *Science* **306**, 666 (2004).
2. F. Bonaccorso, Z. Sun, T. Hasan, A. C. Ferrari, *Nat. Photon.* **4**, 611 (2010).
3. K. S. Novoselov *et al*., *Nature* **490**, 192 (2012).
4. A. N. Grigorenko, M. Polini, K. S. Novoselov, *Nat. Photon.* **6**, 749 (2012).
5. Y. M. Lin *et al*., *Science* **327**, 662 (2010).
6. T. Li *et al*., *Phys. Rev. Lett.* **108**, 167401 (2012).
7. P. Tassin, T. Koschny, M. Kafesaki, C. M. Soukoulis, *Nat. Photon.* **6**, 259 (2012).
8. H. Yan *et al*., *Nat. Nanotechnol.* **7**, 330 (2012).
9. J. Chen *et al*., *Nature* **487**, 77 (2012).
10. Z. Fei *et al*., *Nature* **487**, 82 (2012).
11. Z. Q. Li *et al*., *Nat. Phys.* **4**, 532 (2008).
12. A. Vakil, N. Engheta, *Science* **332**, 1291 (2011).
13. F. H. L. Koppens, D. E. Chang, F. J. García de Abajo, *Nano Lett.* **11**, 3370 (2011).
14. J.-H. Chen, C. Jang, S. Xiao, M. Ishigami, M. S. Fuhrer, *Nat. Nanotechnol.* **3**, 206 (2008).
15. See supplementary materials on *Science* Online.

Acknowledgments: Supported by Ames Laboratory, U.S. Department of Energy (Basic Energy Sciences, Division of Materials Sciences and Engineering), under contract DE-AC02-07CH1358; by European Research Council grant no. 320081 (PHOTOMETA); and by Office of Naval Research, award no. N00014-10-1-0925.

Supplementary Materials

www.sciencemag.org/cgi/content/full/341/6146/620/DC1
Table S1
References

10.1126/science.1242253

TRANSCRIPTION

Flashing a Light on the Spatial Organization of Transcription

Transient and highly dynamic clusters of RNA polymerase II form during the initiation phase of transcription.

Colin Rickman[1,2] and Wendy A. Bickmore[2,3]

It is surprising that the question of how transcription occurs in the eukaryotic cell nucleus is still a matter of controversy, given that it is such a basic cellular process. Conventional imaging of transcription sites, RNA polymerase II (Pol II), and active genes suggests that transcription occurs at discrete places in the nucleus, termed transcription factories. What has not been clear is whether these sites are preassembled structures that prefigure function and to which genes must then move to be transcribed, or whether they are self-organizing zones that form at active gene loci during the process of gene expression (*1*). One problem in resolving these issues has been the lack of information about the formation and stability of transcription factories in living cells—which could not be detected by conventional light microscopy with green fluorescent protein (GFP)–tagged Pol II (*2*). On page 664 of this issue, Cisse *et al*. (*3*) surmount this problem by using single-molecule light microscopy to determine the spatiotemporal organization of Pol II in the nucleus. Their observations of the formation of short-lived Pol II clusters that respond to transcriptional stimuli provide compelling evidence against the idea of preassembled stable transcription factories.

Cisse and colleagues expressed an α-amanitin–resistant form of the Pol II catalytic subunit (RPB1), fused to the photoswitchable fluorescent protein Dendra2, in a human cell line in which endogenous Pol II was destroyed with α-amanitin (*4*). Photoactivation localization microscopy (PALM) (*5*) was then used to examine Pol II at single-molecule resolution. By photoswitching a small subset of the Dendra2–Pol II molecules (see the figure, panel A), their emitted light can be spatially resolved and their molecular position determined with high precision (on the order of tens of nanometers). However, a major limitation of PALM is that all depth (axial) information is lost in the final data set, commonly limiting its application to the study of events at the cell surface. Cisse *et al*. circumvented this problem by performing PALM in live cells and analyzing both the size and the dynamics of cluster formation. Pair correlation was used to determine the probability of molecules residing at given distances from each other. This demonstrated the presence of Pol II clusters with an estimated size of ~100 nm,

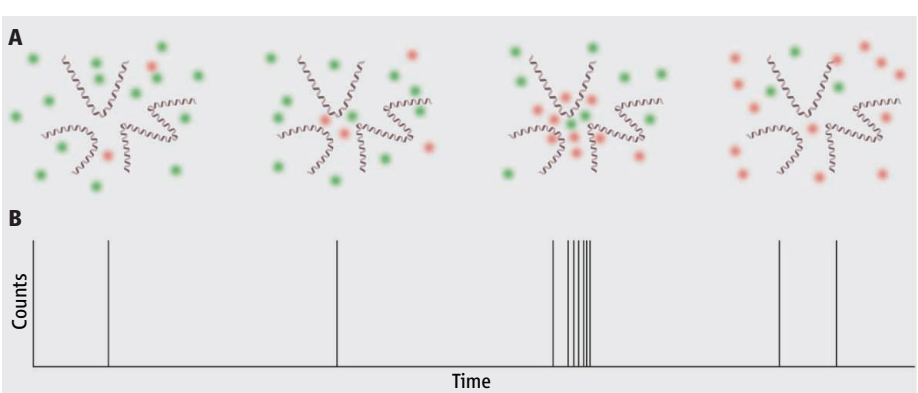

Clustering to transcribe. (**A**) Cartoon showing four frames taken from a time series of images of Dendra2–Pol II molecules (small circles) in a small genomic region before (green) and after (red) photoswitching. In the third frame from the left, the sudden appearance of a large number of photoswitched molecules in the imaged area indicates the formation of a Pol II cluster. That this does not continue into the fourth frame, even though photoswitching continues generally, indicates cluster dispersal. (**B**) Graph showing the detection (vertical lines) of Dendra2–Pol II photoswitching events per frame that might be seen from the images in (A); the temporally correlated high detection counts in the third frame indicate cluster formation.

[1]Institute of Biological Chemistry, Biophysics and Bioengineering, Heriot-Watt University, Edinburgh EH14 4AS, UK. [2]Edinburgh Super-Resolution Imaging Consortium, www.esric.org. [3]MRC Human Genetics Unit, Institute of Genetics and Molecular Medicine, University of Edinburgh, Edinburgh EH4 2XU, UK. E-mail: wendy.bickmore@igmm.ed.ac.uk

www.sciencemag.org/cgi/content/full/341/6146/620/DC1

Supplementary Materials for

Graphene for Terahertz Applications

Philippe Tassin, Thomas Koschny, Costas M. Soukoulis*

*Corresponding author. E-mail: soukoulis@ameslab.gov

Published 9 August 2013, *Science* **341**, 620 (2013)
DOI: 10.1126/science.1242253

This PDF file includes:

Table S1
References

Table S1a. Sheet conductivity, resistivity and inductivity of graphene obtained from direct experimental terahertz measurements (multiple sources). The complex sheet conductivity σ is given by way of the collision frequency γ and the Drude weight α as in $\sigma = \alpha / (\gamma - i\omega)$, where ω is the angular frequency. (Blue data points in Fig. 1.)

	α (GHz/Ω)	γ (THz)	Resistivity (Ω)	Inductivity (Ω/THz)
Yan *et al.* (1)	76.0	9.80	129	13
Yan *et al.* (1)	44.2	13.6	308	23
Kim *et al.* (2)	52.2	17.9	343	19
Yan *et al.* (1)	44.2	17.3	391	23
Kim *et al.* (2)	47.6	18.8	395	21
Yan *et al.* (3)	42.0	17.1	407	24
Kim *et al.* (2)	35.8	17.9	500	28
Kim *et al.* (2)	32.4	17.9	552	31
Chen *et al.* (4)	47.5	30.1	634	21
Yan *et al.* (3)	28.8	19.2	667	35
Horng *et al.* (5)	27.6	20.7	750	36
Lee *et al.* (6)	21.0	17.9	852	48
Lin *et al.* (7)	10.1	9.90	980	99
Rouhi *et al.* (8)	17.8	20.0	1124	56
Fei *et al.* (9)	15.9	22.7	1428	63
Li *et al.* (10)	19.9	29.4	1477	50
Horng *et al.* (5)	17.9	36.6	2045	56
Yan *et al.* (3)	14.6	50.7	3473	68
Kim *et al.* (2)	5.39	22.6	4193	186

Table S1b. Sheet conductivity, resistivity and inductivity of graphene obtained from (DC) transport measurements (multiple sources). The complex sheet conductivity σ is given by way of the collision frequency γ and the Drude weight α as in $\sigma = \alpha / (\gamma - i\,\omega)$, where ω is the angular frequency. (Green data points in Fig. 1.)

	α (GHz/Ω)	γ (THz)	Resistivity (Ω)	Inductivity (Ω/THz)
Efetov *et al.* (11)	167	5.99	36	6
Bolotin *et al.* (12)	6.80	0.917	135	147
Ye *et al.* (13)	66.7	11.2	167	15
Ye *et al.* (13)	100	21.3	222	10
Efetov *et al.* (11)	47.6	11.0	230	21
Pallecchi *et al.* (14)	23.8	11.1	470	42
Bolotin *et al.* (12)	6.80	7.52	1109	147
Pallecchi *et al.* (14)	23.8	33.3	1400	42

Table S1c. Sheet conductivity, resistivity and inductivity of graphene assumed in a number of theoretical studies exploring terahertz graphene devices. The complex sheet conductivity σ is given by way of the collision frequency γ and the Drude weight α as in $\sigma = \alpha / (\gamma - i\,\omega)$, where ω is the angular frequency.
(Red data points in Fig. 1.)

	α (GHz/Ω)	γ (THz)	Resistivity (Ω)	Inductivity (Ω/THz)
Li *et al.* (15)	178	2.00	11	6
Alaee *et al.* (16)	23.7	0.305	13	42
Gao *et al.* (17)	76.0	1.89	25	13
Tamagnone *et al.* (18)	23.7	1.00	42	42
Koppens *et al.* (19)	119	10.0	84	8.4
Vakil *et al.* (20)	14.4	2.00	139	69
Iorsh *et al.* (21)	5.20	3.05	587	129
Llatser *et al.* (22)	4.10	10.0	2439	244

References

S1. H. Yan, X. Li, B. Chandra, G. Tulevski, Y. Wu, M. Freitag, W. Zhu, P. Avouris, F. Xia, Tunable infrared plasmonic devices using graphene/insulator stacks. *Nat. Nanotechnol.* **7**, 330–334 (2012). doi:10.1038/nnano.2012.59 Medline

S2. J. Y. Kim, C. Lee, S. Bae, K. S. Kim, B. H. Hong, E. J. Choi, Far-infrared study of substrate-effect on large scale graphene. *Appl. Phys. Lett.* **98**, 201907 (2011). doi:10.1063/1.3590773

S3. H. Yan, F. Xia, W. Zhu, M. Freitag, C. Dimitrakopoulos, A. A. Bol, G. Tulevski, P. Avouris, Infrared spectroscopy of wafer-scale graphene. *ACS Nano* **5**, 9854–9860 (2011). doi:10.1021/nn203506n Medline

S4. J. Chen, M. Badioli, P. Alonso-González, S. Thongrattanasiri, F. Huth, J. Osmond, M. Spasenović, A. Centeno, A. Pesquera, P. Godignon, A. Z. Elorza, N. Camara, F. J. García de Abajo, R. Hillenbrand, F. H. Koppens, Optical nano-imaging of gate-tunable graphene plasmons. *Nature* **487**, 77–81 (2012). Medline

S5. J. Horng, C.-F. Chen, B. Geng, C. Girit, Y. Zhang, Z. Hao, H. A. Bechtel, M. Martin, A. Zettl, M. F. Crommie, Y. R. Shen, F. Wang, Drude conductivity of Dirac fermions in graphene. *Phys. Rev. B* **83**, 165113 (2011). doi:10.1103/PhysRevB.83.165113

S6. C. Lee, J. Y. Kim, S. Bae, K. S. Kim, B. H. Hong, E. J. Choi, Optical response of large scale single layer graphene. *Appl. Phys. Lett.* **98**, 071905 (2011). doi:10.1063/1.3555425

S7. I.-T. Lin, J.-M. Liu, K.-Y. Shi, P.-S. Tseng, K.-H. Wu, C.-W. Luo, L.-J. Li, Terahertz optical properties of multilayer graphene: Experimental observation of strong dependence on stacking arrangements and misorientation angles. *Phys. Rev. B* **86**, 235446 (2012). doi:10.1103/PhysRevB.86.235446

S8. N. Rouhi, S. Capdevila, D. Jain, K. Zand, Y. Y. Wang, E. Brown, L. Jofre, P. Burke, Terahertz graphene optics. *Nano Res.* **5**, 667–678 (2012). doi:10.1007/s12274-012-0251-0

S9. Z. Fei, A. S. Rodin, G. O. Andreev, W. Bao, A. S. McLeod, M. Wagner, L. M. Zhang, Z. Zhao, M. Thiemens, G. Dominguez, M. M. Fogler, A. H. Castro Neto, C. N. Lau, F. Keilmann, D. N. Basov, Gate-tuning of graphene plasmons revealed by infrared nano-imaging. *Nature* **487**, 82–85 (2012). Medline

S10. Z. Q. Li, E. A. Henriksen, Z. Jiang, Z. Hao, M. C. Martin, P. Kim, H. L. Stormer, D. N. Basov, Dirac charge dynamics in graphene by infrared spectroscopy. *Nat. Phys.* **4**, 532–535 (2008). doi:10.1038/nphys989

S11. D. K. Efetov, P. Kim, Controlling electron-phonon interactions in graphene at ultrahigh carrier densities. *Phys. Rev. Lett.* **105**, 256805 (2010). doi:10.1103/PhysRevLett.105.256805 Medline

S12. K. I. Bolotin, K. J. Sikes, Z. Jiang, M. Klima, G. Fudenberg, J. Hone, P. Kim, H. L. Stormer, Ultrahigh electron mobility in suspended graphene. *Solid State Commun.* **146**, 351–355 (2008). doi:10.1016/j.ssc.2008.02.024

S13. J. Ye, M. F. Craciun, M. Koshino, S. Russo, S. Inoue, H. Yuan, H. Shimotani, A. F. Morpurgo, Y. Iwasa, Accessing the transport properties of graphene and its multilayers at high carrier density. *Proc. Natl. Acad. Sci. U.S.A.* **108**, 13002–13006 (2011). doi:10.1073/pnas.1018388108 Medline

S14. E. Pallecchi, A. C. Betz, J. Chaste, G. Fève, B. Huard, T. Kontos, J.-M. Berroir, B. Plaçais, Transport scattering time probed through rf admittance of a graphene capacitor. *Phys. Rev. B* **83**, 125408 (2011). doi:10.1103/PhysRevB.83.125408

S15. P. Li, T. Taubner, Broadband subwavelength imaging using a tunable graphene-lens. *ACS Nano* **6**, 10107–10114 (2012). doi:10.1021/nn303845a Medline

S16. R. Alaee, M. Farhat, C. Rockstuhl, F. Lederer, A perfect absorber made of a graphene micro-ribbon metamaterial. *Opt. Express* **20**, 28017–28024 (2012). doi:10.1364/OE.20.028017 Medline

S17. W. Gao, J. Shu, C. Qiu, Q. Xu, Excitation of plasmonic waves in graphene by guided-mode resonances. *ACS Nano* **6**, 7806–7813 (2012). doi:10.1021/nn301888e Medline

S18. M. Tamagnone, J. S. Gómez-Díaz, J. R. Mosig, J. Perruisseau-Carrier, Reconfigurable terahertz plasmonic antenna concept using a graphene stack. *Appl. Phys. Lett.* **101**, 214102 (2012). doi:10.1063/1.4767338

S19. F. H. Koppens, D. E. Chang, F. J. García de Abajo, Graphene plasmonics: A platform for strong light-matter interactions. *Nano Lett.* **11**, 3370–3377 (2011). doi:10.1021/nl201771h Medline

S20. A. Vakil, N. Engheta, Transformation optics using graphene. *Science* **332**, 1291–1294 (2011). doi:10.1126/science.1202691 Medline

S21. I. V. Iorsh, I. S. Mukhin, I. V. Shadrivov, P. A. Belov, Y. S. Kivshar, Hyperbolic metamaterials based on multilayer graphene structures. *Phys. Rev. B* **87**, 075416 (2013). doi:10.1103/PhysRevB.87.075416

S22. I. Llatser, C. Kremers, A. Cabellos-Aparicio, J. M. Jornet, E. Alarcón, D. N. Chigrin, Graphene-based nano-patch antenna for terahertz radiation. *Photon. Nanostruct. Fund. Appl.* **10**, 353–358 (2012). doi:10.1016/j.photonics.2012.05.011